Membrane and Water Treatment, *Vol. 17, No. 2 (2026) 145-168*
https://doi.org/10.12989/mwt.2026.17.2.145

Development and performance of chemically treated PVDF hollow fiber membrane under UV post-treatment

Eman S. Sayed*[1], Hayam F. Shaalan[1], Magda I. Marzouk[2], Heba A. Hani[1]

[1]*Chemical Engineering and Pilot Plant Department, Engineering and Renewable Energy Research Institute, National Research Centre, El-Buhouth Street, Dokki, Giza, Egypt*
[2]*Organic Chemistry Department, Faculty of Science, Ain Shams University, 11566, Cairo, Egypt*

(Received October 14, 2025, Revised January 19, 2026, Accepted January 29, 2026)

Abstract. This study investigates the effects of ultraviolet (UV) irradiation on the structural, chemical, and performance characteristics of polyvinylidene fluoride (PVDF) hollow fiber membranes (HFMs), with and without chemical treatment using hydrogen peroxide (H_2O_2) or polyethylene glycol (PEG). Membranes were exposed to UV light for 10, 20, and 30 minutes. Characterization techniques including SEM, FTIR, EDS, NMR, and AFM revealed that short-term UV treatment preserved the chemical integrity of the membranes and caused no significant surface damage, especially in chemically pretreated samples. PEG and H_2O_2 treatments enhanced membrane resistance to UV-induced degradation. Surface hydrophilicity improved with UV exposure, as indicated by reduced water contact angles and increased porosity. The treated membranes exhibited increased permeability 52.6 LMH to 82.3 LMH after 30 minutes of UV exposure, especially in H_2O_2-modified samples, while maintaining Methylene blue (MB) rejection of 75%. In contrast, PEG-modified membranes showed reduced permeability (from 49.8 LMH to 29.2 LMH) with UV exposure due to partial pore blocking. Mechanical strength varied with treatment, showing slight improvements in H_2O_2-treated samples and reductions in raw and PEG-treated ones. These findings demonstrate that UV post-treatment, especially when combined with H_2O_2, provides a clean and effective modification route to enhance PVDF HFMs, leading to improved hydrophilicity, permeability, and stability for water treatment applications.

Keywords: characterization; hollow fiber membrane; performance; PVDF; UV- post treatment

1. Introduction

Hollow fibre membranes (HFMs) are of substantial economic interest in separation and purification processes, particularly in wastewater treatment, industrial, and biomedical applications [1-8]. Compared with flat-sheet or tubular membranes, HFMs offer several avdvantages, including high surface-to-volume ratio, ease of operation, reduced fouling, and simple integration into flow systems [2]. They have been successfully applied in reverse osmosis (RO), nanofiltration (NF), and ultrafiltration (UF) [9, 10]. Polyvinylidene fluoride (PVDF) is one of the most widely used polymers for fabricating HFMs due to its excellent mechanical, thermal, and chemical resistance. However, its poor wettability and tendency toward organic fouling limit its performance in aqueous applications [11-13]. Various approaches, including chemical, mechanical, electrical, and

*Corresponding author, Ph.D., E-mail: emanamoonaa15@gmail.com; Emansayed1522@gmail.com

ISSN: 2005-8624 (Print), 2092-7037 (Online)

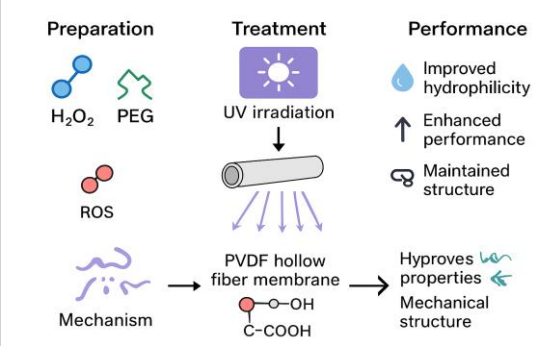

Graphical abstract

hydraulic have been employed to mitigate fouling, with chemical modification and cleaning being the most widely adopted [14-17].

Recently, advanced oxidation processes (AOPs), particularly photocatalytic membranes, have gained attention for their ability to degrade refractory and non-biodegradable compounds [18-20]. Submerged membrane photocatalytic reactors (sMPRs) are especially attractive as they simultaneously purify water and degrade organic pollutants. However, exposure to ultraviolet (UV) light, which drives photocatalysis, can also damage polymeric membranes by inducing chain scission, chemical alterations, and structural degradation [21-27].

Several studies have investigated the UV stability of different polymers, including polymethylmethacrylate (PMMA), Polyvinyl Chloride (PVC), polypropylene (PP), polycarbonate (PC), Polytetrafluoroethylene (PTFE) PVDF and polyacrylonitrile (PAN) and polyethersulfone (PES) [28-32]. While PVDF, PTFE, and PAN showed relatively higher stability during prolonged irradiation, severe degradation such as cracking and surface collapse has also been reported after extended exposure. [33] reported that after 120 h of direct UV exposure, the outer surface layer of PVDF HFMs developed cracks and fractures, and the membrane structure eventually collapsed into powder. Similarly, Rupiasih et al. [23] found that polysulfone (PSf) membranes exposed to UV light (0.28 W/m²) for only 45–60 min exhibited surface cracks and fractures. Furthermore, understanding the aging mechanisms is crucial for ensuring the long-term integrity of modified membranes; for instance, Roubaud et al. [34] investigated the aging of PVDF-PVP-TiO_2 HFMs under UV irradiation, highlighting how structural changes and the degradation of additives can influence the self-cleaning properties and overall membrane lifespan.

While, Jyothi et al. [35] observed that PSf/TiO_2 mixed matrix membranes suffered random cracks after just 40 min of UV exposure. In contrast, Mohamad et al. [36] showed that PES UF membranes coated with TiO_2 and irradiated for 15–30 min (184 W lamp) exhibited enhanced pure water flux and humic acid permeability compared to unirradiated membranes. Kim et al. [37] produced a hybrid thin-film composite (TFC) membrane by enabling TiO_2 nanoparticles to self-assemble through interaction with COOH functional groups. Madaeni et al. [38] reported that the flux of TiO_2-coated poly(aryl sulfone ether) membranes increased significantly after UV irradiation compared to raw membranes. Muchtar et al. [39] investigated the role of a polydopamine layer in improving PVDF membrane resistance to UV irradiation in photocatalytic reactors, although chemical structure changes due to photodegradation were still detected. These studies indicate that UV irradiation significantly alters membrane surfaces, yet few have systematically examined its effect on PVDF HFMs separation performance, microstructure, and chemical

composition. In this context, Polyethylene glycol (PEG) was selected as a surface-modifying agent due to its exceptional hydrophilic nature, biocompatibility, and its ability to reduce organic fouling [40, 41]. The presence of ether oxygen groups in PEG enhances the water affinity of the membrane surface, while its UV-responsive nature facilitates stable interaction and efficient grafting onto the PVDF matrix [42]. Such stable surface attachment is critical for improving the durability and functional performance of modified HFMs under UV exposure.To address this gap, the present study systematically investigates the effects of short-term UV irradiation (10–30 minutes) on PVDF HFMs, with and without preliminary chemical pre-treatments using H_2O_2 and PEG. The membranes were comprehensively characterized in terms of surface morphology, roughness, chemical composition, wettability, porosity, mechanical properties, followed by evaluation of pure water permeability and MB dye rejection. The findings provide insights into the potential of UV-based post-treatment as a clean and non-destructive strategy to improve PVDF HFMs performance for water treatment applications.

2. Materials and methods

2.1 Materials

Polyvinylidene fluoride (PVDF), used as the base polymer, was purchased from Alfa Aeser, Germany. Dimethylacetamide (DMAc) used as the solvent was supplied from Carl-Roth. Polyvinyl pyrrolidone (PVP M.wt. 90k) and Polyvinylidene fluoride-co-hexafluoropropylene (PVDF-CO-HFP average M.wt. 400000-130000) were purchased from Sigma Aldrich used as pore former and a non-solvent additive, respectively. Hydrogen peroxide (H_2O_2) was provided by Luna Co., Ltd, Egypt. Methylene blue dye (MB M.wt. 319.86) was used as feed solution for synthetic dye, purchased from S.d.fine - Chem LTd. NaCL, and Formalin supplied by PIOCHEM laboratory chemicals, Egypt were used as preservative solutions for the base HFMs. Polyethylene glycol (PEG400) was purchased from Sigma Aldrich as used as a hydrophilicity enhancer and surface modifier, as justified in the introduction.

2.2 PVDF HFMs preparation and post-treatment

PVDF HFMs were prepared via the dry/wet phase inversion spinning technique, as previously reported [16, 43-46]. In a typical experiment, the dope composition was prepared by dissolving PVDF (13.6 wt%) in DMAc (78.3 wt %) solvent, PVP K-90 (6.8wt%), and PVDF-CO-HFP (1.36 wt%) were added as a pore former, and a co-polymer additive, respectively. The spun PVDF HFMs were washed thoroughly in RO water. Washed membranes were stored in NaCl, and formalin solution for further analysis and treatment. Raw PVDF HFMs were denoted by (R). Post treated sample with H_2O_2 were carried out at 45°C for 3 hrs in a water bath [16]. Post-treatment using PEG 400 was performed by immersing raw PVDF HFMs in 1% PEG solution for 45 min at 40 °C in a shaking water bath. After treatment, the fibers were removed, thoroughly washed with deionized water, and then dried prior to characterization. The PEG-treated samples were denoted as R_p.

2.3 Ultraviolet-combined treatment of raw, and chemically post-treated samples

The UV irradiation system consisted of a custom-made wooden chamber internally lined with a

Figure 1. Ultraviolet apparatus [47]

2 mm thick silver metal sheet to enhance light reflection. The chamber was equipped with six low-pressure mercury UV lamps (15 W each, wavelength 254 nm, UV-C; El-Gomhoria Co., Egypt), positioned at a fixed distance of 10 cm from the HFMs. Three axial fans (220–240 V, 1.68 W) and a temperature control unit were employed to maintain thermal stability during irradiation. The overall design and operation of the UV system followed the configuration previously reported by [47], as illustrated in Fig. 1.

Based on lamp specifications, irradiation geometry, and literature reported data for comparable UV-C systems, the UV irradiance at the membrane surface is expected to fall within the same order of magnitude (approximately 10^1 mW cm^{-2}). To avoid potential overestimation and ensure reproducibility, UV exposure time (10, 20, and 30 min) was used as the primary comparative parameter rather than absolute irradiance or dose values.

Raw and chemically pretreated PVDF HFMs were prepared according to the procedure reported by [16]. After UV post-treatment, samples were collected at irradiation times of 10, 20, and 30 min for characterization. The membranes were coded as R_{10}, R_{20}, R_{30} (raw PVDF), R_{H10}, R_{H20}, R_{H30} (H_2O_2-treated), and R_{p10}, R_{p20}, and R_{p30} (PEG-treated).

2.4 Characterization

2.4.1 Chemical analysis

Fourier transform Infrared spectroscopy (FTIR)

FTIR analysis was used to identify the chemical structure of raw, and UV post treated PVDF HFMs. Sample were prepared by mixing 1 mg of the samples with 500 mg of KBr (Merck) in an agate mortar using (FT/IR-6100 from A Jasco, Japan detector) infrared spectrophotometer with the transmittance mode with a scanning range of 400 cm-1 to 4000 cm^{-1}.

Proton nuclear magnetic resonance (^{1}H- NMR)

^{1}H-NMR spectra was conducted on A JEOL ECA NMR of raw, and UV post treated PVDF HFMs samples dissolved in dimethyl sulfoxide as solvent (DMSO).

Elemental analysis (EDS)

Elemental analysis of raw, and UV post treated PVDF HFMs were determined using a JOEL JCM-6000 Neoscope desktop scanning electron microscope (SEM) device at a high vacuum of 15 kV. Fibers were cut using a sharp razor and carbon taped to the sample container before being gold-sputtered to boost sample conductivity and produce better pictures.

2.4.2 Surface morphology

Scanning electron microscope (SEM)

The morphological characteristics, and dimensions for raw, and UV post treated PVDF HFMs were determined using the same apparatus mentioned in 2.4.1. To confirm the repeatability of the results, a minimum of six segments from each sample were analyzed and their average inner, outer and wall thickness values were obtained.

Surface Roughness (AFM)

An atomic force microscope (AFM) equipped with a 400X zoom video optical microscope and TT-AFM workshop with 1.5 micron resolution examined the surface topography and roughness for raw, and UV post treated PVDF HFMs. Double-face tape was used to adhere samples to a magnetic plate. Testing was carried out in the vibrating scan mode using a 5 µm x 5 µm scan area. Roughness parameters were calculated using the "Gwidyyon" program. For each sample, six different scan areas were examined (n=6), and the roughness parameters (Ra and Rms) were reported as the mean ± standard deviation to ensure a representative topographical characterization.

2.4.3 Water contact angle (CA°)

The surface hydrophilicity of the raw and UV post-treated PVDF HFMs was evaluated by measuring the water contact angles (CA) using a contact angle goniometer (Model OCA 15EC, Data Physics Instruments GmbH, Germany). To overcome the challenges associated with the curved outer surface of the HFMs, several fiber specimens were aligned parallel and securely fixed onto a glass slide to create a sufficiently flat and stable surface for measurement. The sessile drop method was employed, using a 2-3 µL droplet of deionized water deposited via using a microsyringe. The droplet images were captured using the system's high-resolution CCD camera and analyzed using the SCA 20 software (Data Physics Instruments GmbH). For each membrane sample, the mean value ± standard deviation of five measurements (n=5) taken at different locations was reported to ensure reproducibility and statistical significance.

2.4.4 Porosity and Mean pore size

Total membrane porosity was determined according to its dry-wet weight. Firstly, raw and UV post-treated PVDF HFMs were dried at 60°C and weighed with a precision balance, then impregnated with kerosene for about 24 h and weighed again after wiping the excess kerosene with filter paper 11. The porosity (Ɛ) of the raw and post treated HFMs was calculated using the following Eq. (1): [48, 49].

$$\varepsilon(\%) = \frac{\frac{w_W - w_D}{D_{kerosene}}}{\frac{w_W - w_D}{D_{kerosene}} + \frac{w_D}{D_{polymer}}} * 100 \quad (1)$$

where ε is the membrane porosity (volume %), w_W is the weight of the wet membrane (g), w_D the weight of the dry membrane (g), $D_{kerosene}$ the density of kerosene (0.82 g/cm3), $D_{polymer}$ is the density of polymer (PVDF) (1.78 g/cm^3).

Mean pore size for the raw, and UV post-treated PVDF HFMs sample were determined using pore size distribution analyzer Belsorp Max apparatus (MicrotracBel. Corp.). Adsorptive nitrogen was used at 77 K. Vacuum degree before measurement was 6.95E-4 Pa and standard vapor pressure was 108 kPa.

2.4.5 Mechanical properties

The mechanical characteristics of raw, and UV post treated PVDF HFMs (break stress, break strain and modulus) have been measured using the Tinius Olsen H5kS, a bench top testing machine with a 5N load cell. Tests were conducted at a gauge length of 100 mm and a jog speed of 50 mm/min. For each sample, six fibers were investigated (n=6), and the results were reported as the mean value ± standard deviation to ensure statistical reliability.

2.4.6 Membrane performance tests

The performance of the raw and UV post treated PVDF HFMs samples have been assessed by permeability measurements. For each sample, about 20 hollow fibers were potted in a suitable connection using epoxy resin to form testing modules. The pure water permeability and flux were measured using a permeability test set up provided by "PHILOS Co., Ltd". The pure water flux of the membranes samples was determined using RO water while, rejection was measured using methylene blue dye solution (50 ppm). The pure water flux or permeate flux was subsequently calculated according to the following Eq. (2):

$$F = \frac{V}{A} * \Delta t \tag{2}$$

where V is the volume of the water or solution permeated during the experiment, A represents the effective HF membrane surface area (m^2), and Δt denotes the operation time (h). The rejection (%) is calculated using the following Eq. (3):

$$R = \frac{1 - Cp}{Cf} * 100 \tag{3}$$

where, C_f and C_p are the dye concentration in feed and permeate solutions, respectively. The concentration of dye was determined by UV spectrophotometer (TW80) is a high-performance double beam spectrophotometer available with a fixed (2nm) or variable (0.5, 1, 2, 5nm) spectral bandwidth.

3. Results and discussions

3.1 Effect of UV combined treatment on membrane structure

3.1.1 FTIR

The FTIR spectra of PVDF HFMs after UV irradiation, with and without H_2O_2 and PEG pretreatment, are presented in Fig. 2. As previously reported for the raw (R) and H_2O_2-treated (R_H) membranes [16], these samples are included here for comparison purposes. Comparing the raw sample with chemically post-treated membranes (R_H and R_P) after UV irradiation, no significant chemical changes were observed even after 30 minutes of exposure.

The stretching vibrations of the C–N group and C=O are observed at 1174.7 cm^{-1} and 1658 cm^{-1}, respectively, due to the presence of PVP $(C_6H_9NO)_n$ used as a pore-forming agent in the PVDF HFMs. Increasing UV exposure time did not result in notable changes in the main polymer chains of PVDF, including both the α- and β-phases. Peaks at 763, 876, and 1174 cm^{-1} correspond to the α-phase, while peaks at 839, 1072, 1174, 1275, 1401, and 1494 cm^{-1} are attributed to the β-phase.

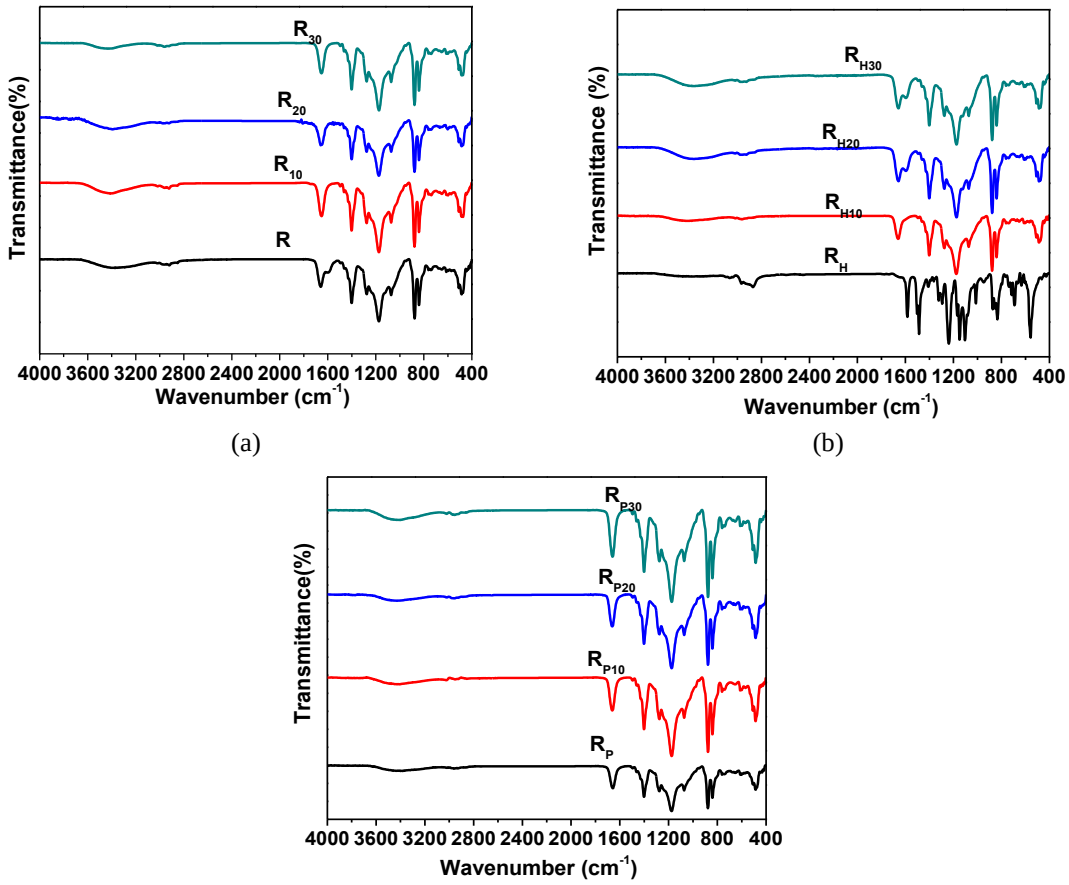

Figure 2. FTIR spectra for raw (a), and UV chemically post-treated PVDF HFMs H2O2 (b), PEG (C) at different UV exposure time

The observed stability can be attributed to the radical scavenging activity of H_2O_2 and PEG functional groups. Hydroxyl groups (-OH, 3200–3600 cm^{-1}) and carboxyl groups (-COOH, 1700–1750 cm^{-1}) act as electron donors, deactivating UV-induced free radicals and thereby preserving the integrity of the PVDF polymer structure [50]. This mechanism helps explain why H_2O_2-treated membranes maintain higher permeability and mechanical strength, while PEG-coated membranes remain protected from surface degradation, although slight pore coverage may reduce permeability.

These findings are consistent with Muchtar et al. [39], who reported no significant changes in IR spectra before and after UV exposure of polydopamine (PDA)-coated PVDF membranes. In contrast, Muchtar et al. [51] reported that long-term UV irradiation of PVDF/TiO_2 HFMs for up to 250 hours caused significant chemical changes and surface degradation.

In conclusion, short duration UV post-treatment preserves the bulk chemical structure of PVDF HFMs without alteration, confirming its role as a clean, non-destructive technique at the molecular level. While the FTIR and EDS results show chemical stability, this treatment allows for targeted

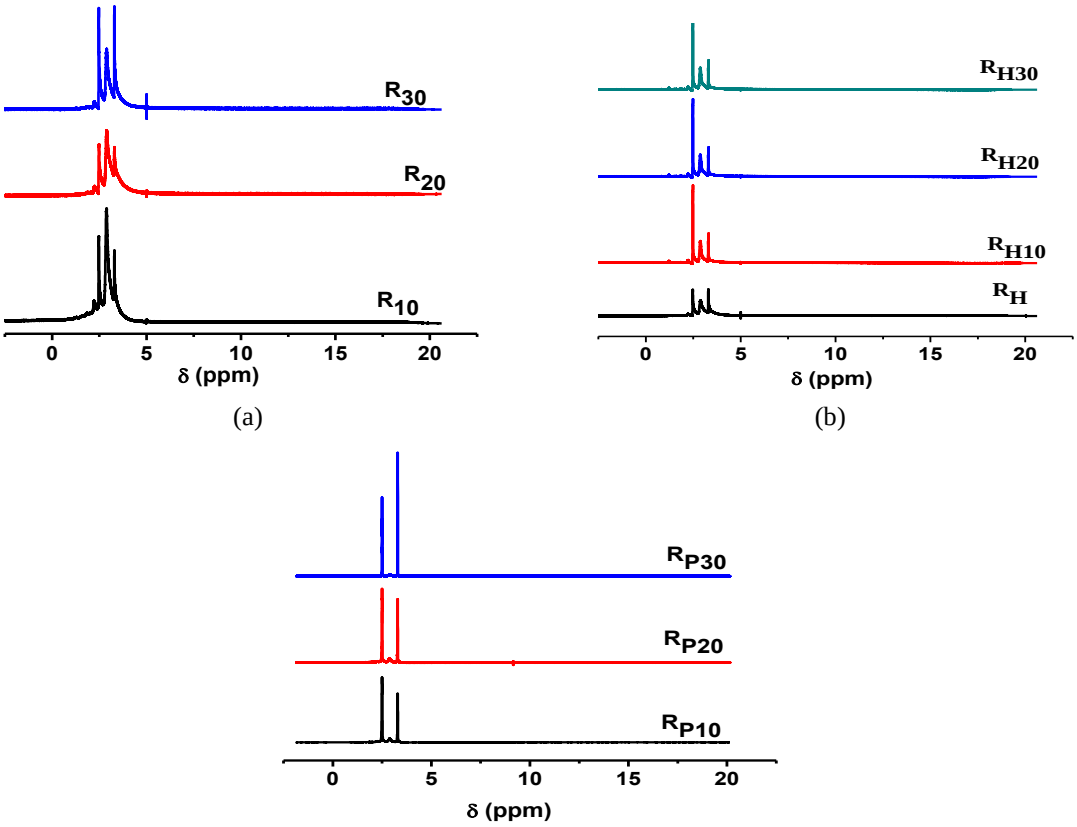

Figure 3. ^{1}H NMR spectra for raw (a), and UV chemically post-treated PVDF HFMs H2O2 (b), PEG (C) at different UV exposure time

structural modulations, such as the significant increases in porosity and pore size observed in subsequent sections. These findings indicate that UV irradiation effectively reconfigures the membrane's physical dimensions while maintaining its essential elemental composition and functional properties like hydrophilicity.

3.1.2 ^{1}H- NMR analysis

The structural characteristics of PVDF HFMs were further analyzed using ^{1}H NMR spectroscopy. The ^{1}H NMR spectra of all prepared UV-irradiated membranes at different exposure times are shown in Fig. 3. As previously reported for the raw (R) and H_2O_2-treated (R_H) membranes [16], these samples are included here for comparison purposes.

All UV-irradiated samples display two characteristic peaks at δ 2.5 ppm and δ 3.1 ppm, corresponding to head-to-head (hh) and head-to-tail (ht) bonding arrangements of the vinylidene fluoride units in the main PVDF polymer chain [52]. For the raw membrane exposed to UV for 30 minutes (R_{30}), a minor new peak at δ 7 ppm was observed Fig. 3(a), indicating slight chemical modification due to UV irradiation, which was not present in the unirradiated raw sample.

In contrast, H_2O_2 and PEG-treated PVDF HFMs showed no significant chemical changes even after 30 minutes of UV exposure. This stability can be attributed to the radical scavenging activity

Table 1. EDS results for raw UV post-treated PVDF HFMs at different UV exposure time

Element (wt%)	R	R_{10}	R_{20}	R_{30}
C	35.5	30.03	30.33	28.90
N	14.17	15.53	16.29	15.41
O	7.54	11.66	9.47	11.67
F	42.77	42.78	43.91	44.02

Table 2. EDS results for H_2O_2 UV chemically post-treated PVDF HFMs at different UV exposure time

Element (wt%)	R_H	R_{H10}	R_{H20}	R_{H30}
C	34.5	32.8	32.7	31.2
N	14.8	17.2	15.7	15.2
O	7.5	8.9	9	9
F	43.3	40.9	40	39.9

Table 3. EDS results for PEG UV chemically post-treated PVDF HFMs at different UV exposure time

Element (wt%)	R_p	R_{p10}	R_{p20}	R_{p30}
C	34.55	29.4	31.5	30.1
N	16.19	16.19	16.4	16.1
O	6.53	11.4	6.1	7.4
F	42.73	42.8	46.2	45.8

of the H_2O_2 and PEG functional groups. Hydroxyl (-OH) groups act as electron donors, deactivating UV-induced free radicals and thereby protecting the polymer backbone [50].

These findings confirm that chemical pretreatment with H_2O_2 or PEG enhances the chemical resistance of PVDF HFMs against UV-induced modifications. The observed NMR stability is consistent with the FTIR results, supporting the conclusion that short term UV irradiation preserves the chemical structure of the membranes. This chemical stability also correlates with the maintained surface morphology observed in SEM images and the sustained hydrophilicity measured by contact angle analysis.

3.1.3 EDS

The elemental composition of PVDF HFMs after UV irradiation at different exposure times was analyzed using EDS, and the results are presented in Table 1-3. The elemental composition of the raw (R) and chemically pretreated membranes (R_H and R_P) prior to UV exposure, previously reported by et al. Sayed [16], is included in the tables to enable direct comparison with UV-irradiated samples.

EDS analysis confirmed that all PVDF HFMs are primarily composed of carbon (C), fluorine (F), oxygen (O), and nitrogen (N). For all UV-irradiated membranes, a decrease in carbon content accompanied by an increase in oxygen content was observed, indicating UV-induced surface oxidation. Oxygen content ranged from approximately 9% to 11.67% for UV-treated samples, compared with about 6.5–7.6% for the untreated membranes (R, R_H, R_P). Fluorine and nitrogen contents exhibited only minor variations across all samples.

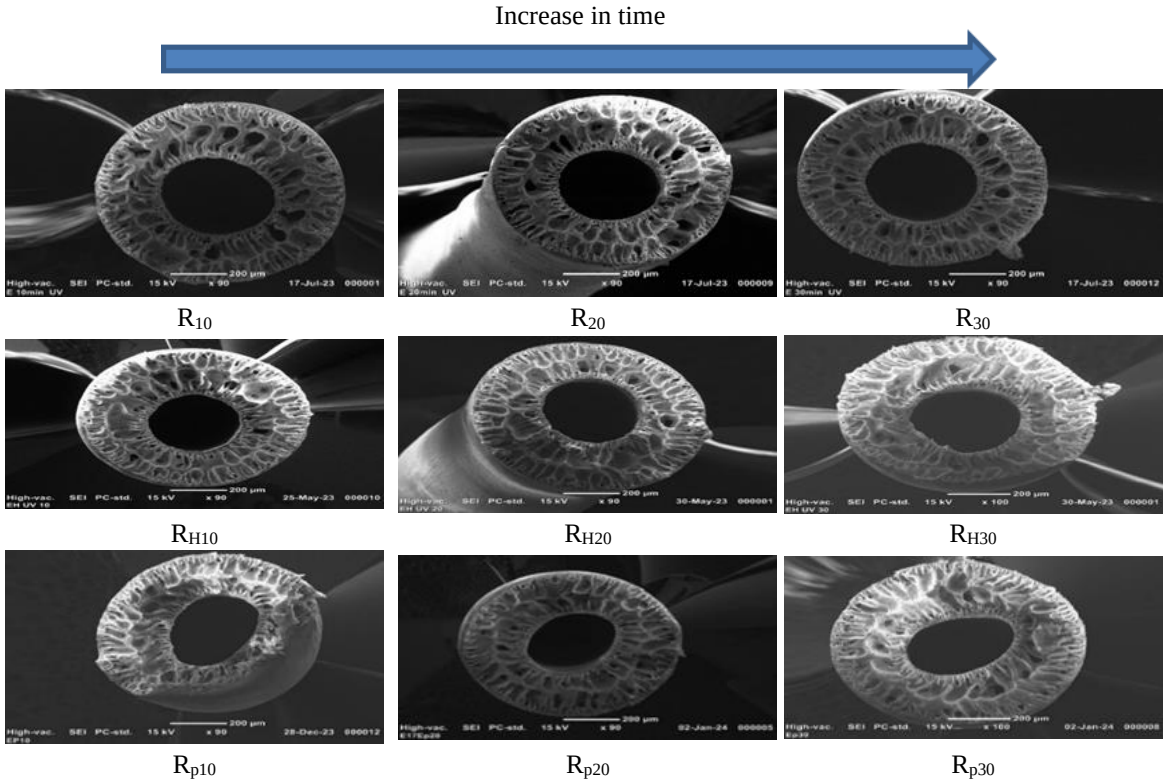

Figure 4. SEM cross section images for UV raw, and chemically post-treated PVDF HFMs at different UV exposure

These results suggest that short-term UV post-treatment (up to 30 min), with or without chemical pretreatment, induces controlled surface chemical modification without pronounced elemental degradation of the PVDF membranes. This interpretation is consistent with FTIR and SEM analyses, which show preserved chemical structure and surface morphology. In contrast, prolonged UV exposure (up to 250 hours) has been reported to cause PVDF degradation [51]. Therefore, the current findings confirm that short-term UV post-treatment effectively maintains surface integrity while enhancing functionalization.

3.2 Effect of UV Combined Treatment on Membrane Surface morphology

3.2.1 SEM

SEM cross-sectional images of PVDF HFMs after UV irradiation for different durations are shown in Fig. 4. As previously reported for the raw (R) and H_2O_2-treated (R_H) membranes [16], these samples are included here for comparison purposes. The cross-section of all membranes displayed an asymmetric double-layer structure with finger-like inner pores and a porous outer layer, consistent with the expected morphology of PVDF hollow fibers.

Outer surface images Fig. 5 reveal that no cracks or fractures formed on the surfaces of raw or chemically treated membranes (R_H, R_P) after up to 30 minutes of UV exposure, indicating that short-term UV irradiation is a non-destructive post-treatment method. For H_2O_2-treated samples

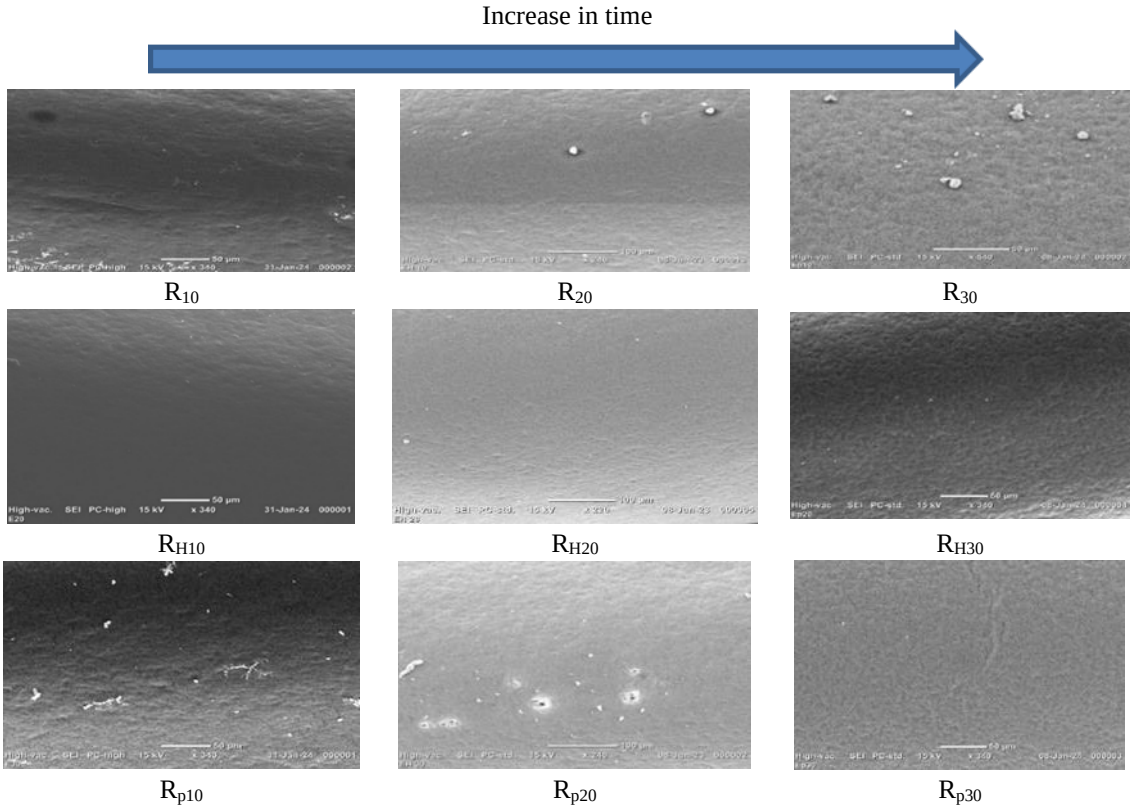

Figure 5. SEM surface images for UV raw, and chemically post-treated PVDF HFMs at different UV exposure

(R_{H10}–R_{H30}), the smooth surface can be attributed to the formation of hydroxyl (-OH) and carboxyl (-COOH) groups during chemical treatment. These functional groups enhance hydrophilicity, reduce surface roughness, and stabilize the polymer chains against UV-induced degradation.

Similarly, PEG-treated membranes (R_{P10}–R_{P30}) maintained smooth surfaces due to the protective PEG coating, which likely absorbs or scatters UV photons, preventing direct polymer degradation. However, slight pore coverage may reduce permeability, as observed in the performance results. Macropores were visible throughout the membrane thickness, confirming that the overall asymmetric structure remains intact even after UV exposure.

Membrane wall thickness exhibited variations after 30 minutes of UV irradiation. While a slight decrease was observed for raw and H_2O_2 -treated membranes (from 252 µm and 258 µm to 243 µm and 251 µm, respectively), the PEG-treated membranes showed a significant reduction in wall thickness, decreasing from 297.8 µm to 238 µm (a 20% reduction). This pronounced decrease in the R_P group could be related to the etching effect of the chemical treatment or polymer chain relaxation and surface compaction under UV energy.

These results align with Bilongo et al. [53] who reported that short-term UV can induce beneficial surface modifications without altering cross-sectional morphology, but differ from Dzinun et al. [54], who found that prolonged UV exposure (30 days) causes surface cracks and polymer degradation for TiO_2/PVDF HFMs. The results align with FTIR, EDS, and contact angle

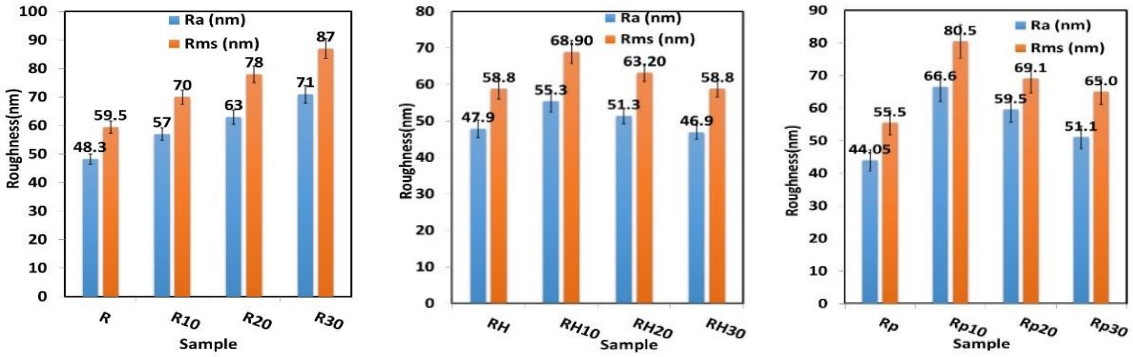

(a) (b) (c)

Figure 6. Surface roughness values for UV raw (a), and UV chemically post-treated PVDF HFMs H_2O_2 (b), PEG (C) at different UV exposure time. Data are presented as mean ± SD (n=6)

analyses, confirming that short-term UV irradiation maintains chemical integrity, surface structure, and hydrophilicity, while H_2O_2 and PEG treatments provide additional stabilization and protection against UV-induced damage.

3.2.2 AFM

The surface topography and roughness of PVDF HFMs after UV post-treatment were investigated using AFM, and the results are presented as Ra and Rms values along with 3D images in Fig. 6, 7. As previously reported for the raw (R) and H_2O_2-treated (R_H) membranes [16], these samples are included here for comparison purposes.

It was observed that short-term UV post-treatment increased the surface roughness of the raw PVDF HFMs. The roughness of the raw membranes increased proportionally with UV exposure time, reaching a maximum Ra value of 71 ± 3.1 nm after 30 minutes, compared to 48.3 ±1.8 nm for the untreated raw PVDF HFM. In contrast, H_2O_2- and PEG-treated membranes exhibited decreased surface roughness with increasing UV exposure times, reaching minimum Ra values of 46.9 ± 1.9 nm and 51.1 ± 3.5 nm after 30 minutes, respectively.

This behavior is attributed to the introduction of hydrophilic functional groups (-OH and -COOH) on the membrane surface during chemical pretreatment. These groups enhance hydrophilicity, reduce surface roughness, and stabilize the membrane against UV-induced damage, consistent with the observed FTIR and EDS results. The reduction in roughness for chemically treated membranes suggests that H_2O_2 and PEG effectively protect the membrane surface while maintaining the functional morphology.

In comparison, prolonged UV exposure on PVDF dual-layer HF membranes with nanoparticles (NPs) over 30 days led to a significant increase in surface roughness from 35.9 nm to 97.4 nm [54]. Such overexposure can generate a rough, brittle surface, negatively affecting mechanical properties and long-term membrane stability. In the current study, short-term UV irradiation combined with chemical pretreatment avoids such detrimental effects, maintaining surface integrity while slightly enhancing hydrophilicity.

Furthermore, the slight increase or decrease in surface roughness influences the contact angle, as roughness amplifies the effect of surface hydrophilicity, leading to a further reduction in water contact angle, consistent with the contact angle measurements described in section 3.3.

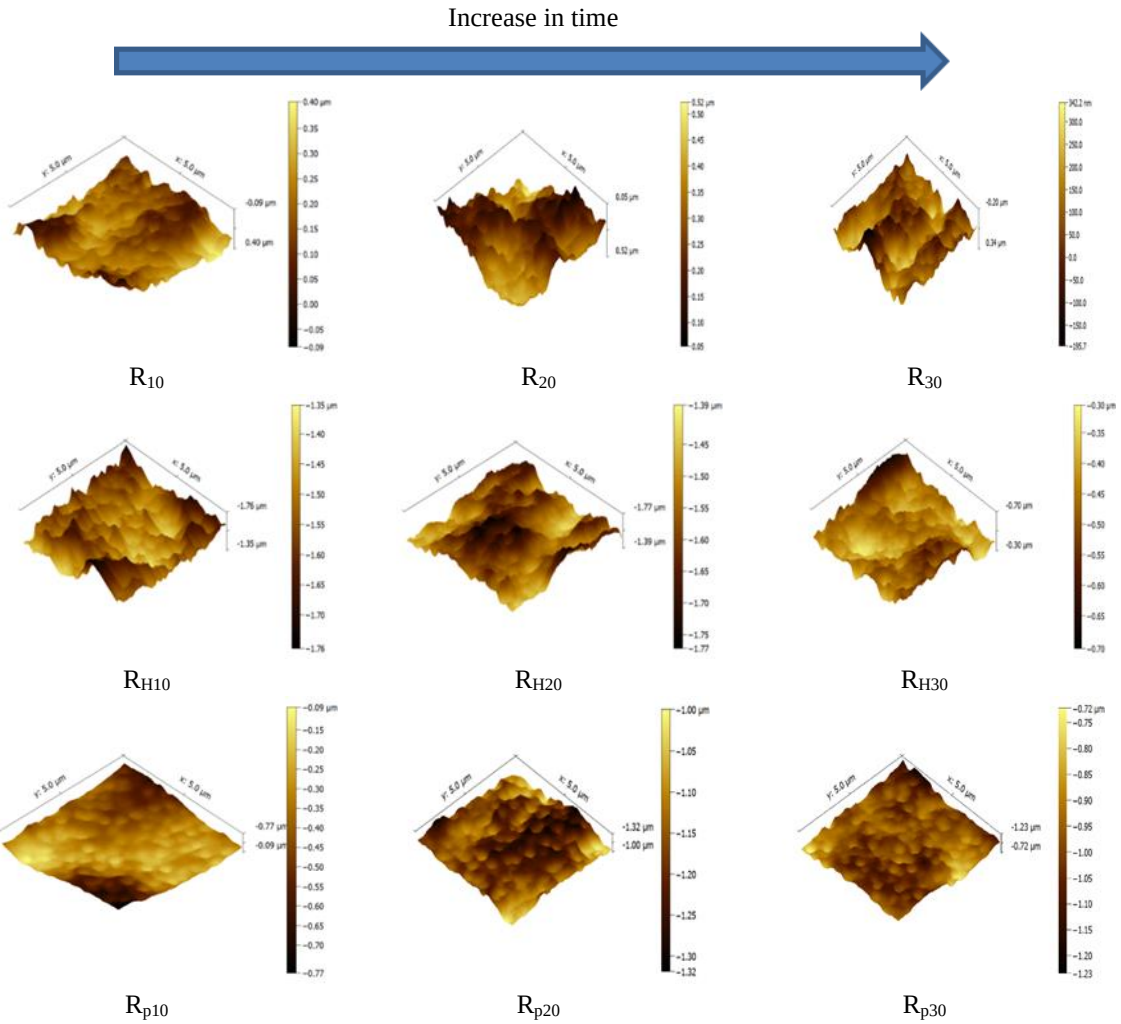

Figure 7. 3D images for UV raw, and chemically post-treated PVDF HFMs at different UV exposure time

3.3 Water contact angle

The water contact angle (CA) is a crucial parameter for predicting the wetting ability, water penetration capacity, and fouling behavior of membranes [55]. The effect of UV irradiation on the water contact angle of PVDF HFMs at different exposure times is shown in Fig. 8. As previously reported for the raw (R) and H_2O_2-treated (R_H) membranes [16], these samples are included here for comparison purposes.

Before UV treatment, the contact angles of the raw, H_2O_2-treated, and PEG-treated PVDF HFMs were 98°± 2.3°, 81.4°± 0.65°, and 80 ± 0.62°, respectively. After UV exposure, the contact angle decreased for all samples, indicating enhanced surface hydrophilicity. For the raw membranes, the contact angle decreased from 98°± 2.3° to 78.6°± 0.54°, while for H_2O_2-treated membranes it decreased slightly from 81°±0.61 ° to 79.9° ± 0.62°, and for PEG-treated membranes it decreased more significantly from 80°± 0.62° to 71°± 0.69°. This decrease in contact angle can be

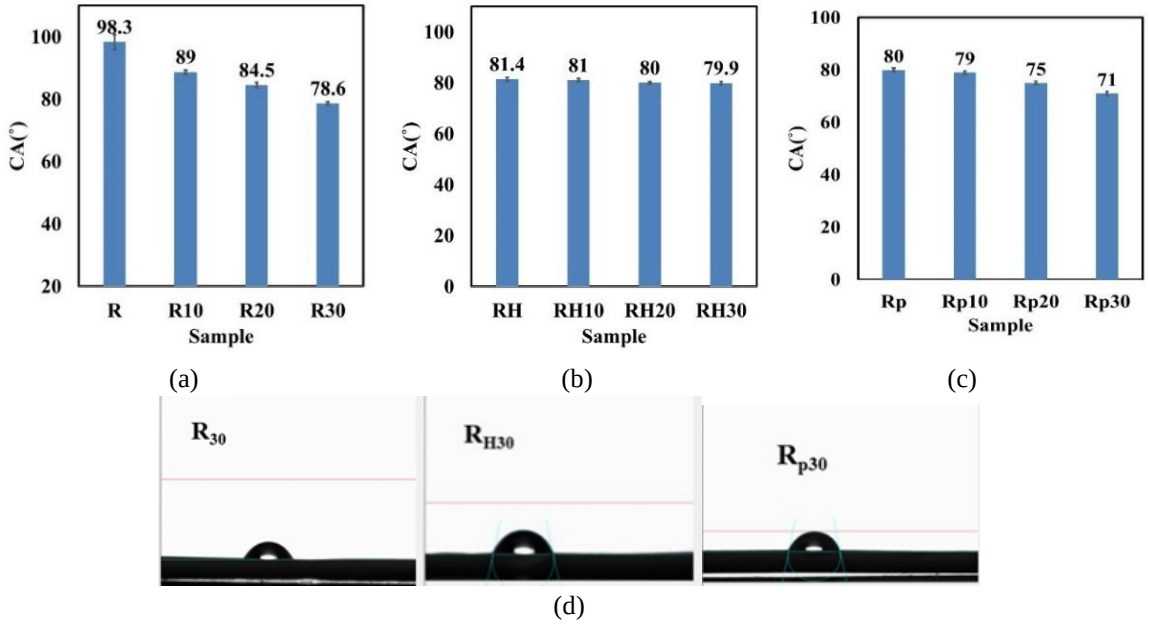

Figure 8. Water contact angles for UV raw (a), and UV chemically post-treated PVDF HFMs H_2O_2 (b), PEG (c) at different UV exposure time, representative sessile drop images for selected samples (R_{30},R_{H30},R_{p30}) (d). Error bars represent the standard deviation (SD) for n=5 measurements

attributed to the UV-induced generation of reactive oxygen species, which promote the formation of polar functional groups such as hydroxyl (-OH), carbonyl (-C=O), and carboxyl (-COOH) on the PVDF surface. These groups increase the surface energy, improving wettability and water affinity.

Similar trends have been reported in the literature. Wang et al. [56] demonstrated increased hydrophilicity through UV-induced grafting of 2-hydroxyethylacrylate onto PS HFMs, while Mohamad et al. [36] observed a decrease in water contact angle with increasing UV irradiation time on PES UF TiO_2-coated membranes. Conversely, prolonged UV exposure may lead to surface degradation or excessive oxidation, resulting in cracks or surface defects, which can increase the contact angle, as reported by [31], [53- 57].

In conclusion, short-term UV irradiation moderately reduces the water contact angle of PVDF HFMs, enhancing hydrophilicity due to the introduction of oxygen-containing functional groups and changes in surface morphology. This improvement in hydrophilicity is consistent with AFM and SEM observations and is expected to enhance membrane performance in terms of water permeability and fouling resistance.

3.4 Mechanical properties.

The mechanical properties of raw (R), H_2O_2-treated (R_H), PEG-treated (R_P), and UV post-treated PVDF HFMs were evaluated and are presented in Tables 4-6**,** respectively. As previously reported for the raw and H_2O_2-treated membranes [16], these samples are included here for comparison purposes. The H_2O_2-treated membranes showed an increase in both break strain and

Table 4. Mechanical properties for raw UV post-treated PVDF HFMs at different UV exposure time

Sample	Break Strain (%)	Break Stress (MPa)	Young's Modulus (MPa)
R	34.5 ± 9.90	1.13± 0.06	19.3± 5.43
R_{10}	24.1 ± 1.46	1.03± 0.04	28.5± 3.85
R_{20}	19.1 ± 1.37	0.91± 0.01	26± 2.91
R_{30}	21.4 ± 3.00	1.01± 0.008	28.4± 3.56

Data are presented as mean ± standard deviation (n=6)

Table 5. Mechanical properties for UV H_2O_2 chemically post-treated PVDF HFMs at different UV exposure time

Sample	Break Strain (%)	Break Stress (MPa)	Young's Modulus (MPa)
R_H	34.8 ± 11.4	1.03± 0.05	22.1± 1.46
R_{H10}	40.3 ±8.2	1.14± 0.04	20.4± 1.11
R_{H20}	39.3 ± 9.3	1.16± 0.03	20.2± 1.79
R_{H30}	39.9 ± 9.4	1.09± 0.02	18± 1.54

Data are presented as mean ± standard deviation (n=6)

Table 6. Mechanical properties for UV PEG chemically post-treated PVDF HFMs at different UV exposure time

Sample	Break Strain (%)	Break Stress (MPa)	Young's Modulus (MPa)
R_p	78.6 ± 4.4	1.38 ± 0.018	29.5± 2.65
R_{p10}	80 ± 12.1	1.3 ± 0.05	23.2± 7.89
R_{p20}	68.8 ± 14.4	1.41 ± 0.04	33.4 ± 1.54
R_{p30}	76.7± 4.9	1.45 ±0.02	28.6 ± 10.80

Data are presented as mean ± standard deviation (n=6)

break stress after UV exposure, whereas raw and PEG-treated membranes exhibited slight reductions, consistent with earlier observations.

For H_2O_2-treated membranes, UV irradiation up to 30 minutes led to an increase in break strain from 34.8% ± 11.4 % to 39.9% ± 9.4% and a slight increase in break stress from 1.03 MPa ± 0.05 MPa to 1.09 MPa ± 0.02 MPa. This improvement is likely due to partial crosslinking between polymer chains induced by UV irradiation, which enhances the polymer network's elasticity and strain capacity. In contrast, the raw and PEG-treated PVDF HFMs experienced a reduction in break strain with increasing UV exposure time. For the raw membranes, this is likely due to the absence of stabilizing functional groups, making them more susceptible to UV-induced structural changes. As for the PEG-treated membranes, this reduction is further intensified by the significant 20% reduction in wall thickness (from 298 µm to 238 µm), as discussed in Section 3.2.1. This thinning, combined with potential pore-blocking effects, reduces the effective cross-sectional area and the polymer network's ability to withstand tensile loads, leading to the observed decline in mechanical integrity shown in Table 6.

These findings align with previous studies Lee et al. [51] reported that the tensile strength of PVDF membranes moderately decreased with prolonged UV exposure, negatively impacting overall membrane stability. Similarly, Dzinun et al. [54] observed that the tensile strength at break

of raw PVDF membranes decreased by over 40% after three days of UV irradiation, and by 60% after five days, primarily due to surface cracks and delamination. In contrast, PDA-coated PVDF membranes exhibited only a 7% reduction in tensile strength after three days and remained nearly constant after five days, indicating that chemical or surface modification can effectively protect the membranes from severe UV-induced mechanical degradation [39].

Overall, these results demonstrate that UV post-treatment, particularly when combined with H_2O_2 pretreatment, can enhance the mechanical performance of PVDF HFMs by stabilizing polymer chains and preventing significant structural damage. Conversely, raw or PEG-coated membranes are more vulnerable to UV-induced weakening, highlighting the importance of chemical stabilization to preserve both mechanical and functional properties under UV exposure. These observations are consistent with the bulk chemical stability (FTIR, NMR) and the targeted structural modulations (SEM, AFM, and pore size analysis) discussed in previous sections, providing a comprehensive understanding of the effects of UV post-treatment on PVDF HFMs.

3.5 Membrane porosity and Mean pore diameter

The effects of UV exposure time on membrane porosity and mean pore diameter were evaluated for raw (R) and chemically post-treated PVDF HFMs with H_2O_2 (R_H) and PEG (R_P), as shown in Fig. 9. As previously reported for raw and H_2O_2-treated membranes [16], these samples are included here for comparison purposes.

The results indicate that UV exposure affects each treatment type differently.While the raw PVDF membrane showed relatively stable porosity remained at approximately 90.5%, the chemically treated membranes exhibited significant structural alterations. In contrast, H_2O_2-treated membranes showed pronounced changes: porosity increased from 91% to 95%, while the mean pore diameter expanded substantially from 10.93 nm to 25.9 nm after 30 minutes of UV exposure. Similarly, PEG-treated membranes exhibited a notable increase in porosity from 88.6% to 92%, with the mean pore diameter increasing consistently from 6.23 nm to 19.34 nm . These substantial increases in both pore size and porosity demonstrate that UV post-treatment, especially when combined with chemical agents, effectively modulates the membrane's physical structure.

These observations demonstrate that UV irradiation impacts membrane structure in a treatment-dependent manner. The H_2O_2-treated membranes show significant porosity enhancement and pore enlargement, likely due to UV-induced formation of hydrophilic functional groups (-OH, -COOH) that facilitate polymer chain relaxation and pore opening. While, the raw membranes maintain stable porosity, the PEG-treated membranes exhibit moderate porosity increase with some pore size stabilization, likely due to the protective effect of the PEG layer.

These findings are consistent with previous reports Siang et al. [33] and Rupiasih et al. [23] observed that direct UV exposure of PVDF and PS HFMs for prolonged durations (40–120 hours) led to the appearance of surface cracks and fractures, resulting in increased pore size. In the present study, the short-term UV exposure did not cause visible cracks or severe degradation, confirming that UV post-treatment is a non-destructive method for modulating membrane porosity and pore dimensions while maintaining the overall mechanical and structural stability of the fibers.

Based on the comprehensive characterization results (FTIR, NMR, SEM, EDS, AFM, contact angle, and mechanical properties), UV post-treatment was found to induce controlled structural and surface chemical modifications in the PVDF HFMs. While the overall fiber integrity was preserved, measurable changes in surface porosity, pore size, and wall thickness were observed, particularly for the H_2O_2- and PEG-treated membranes. Accordingly, performance evaluation,

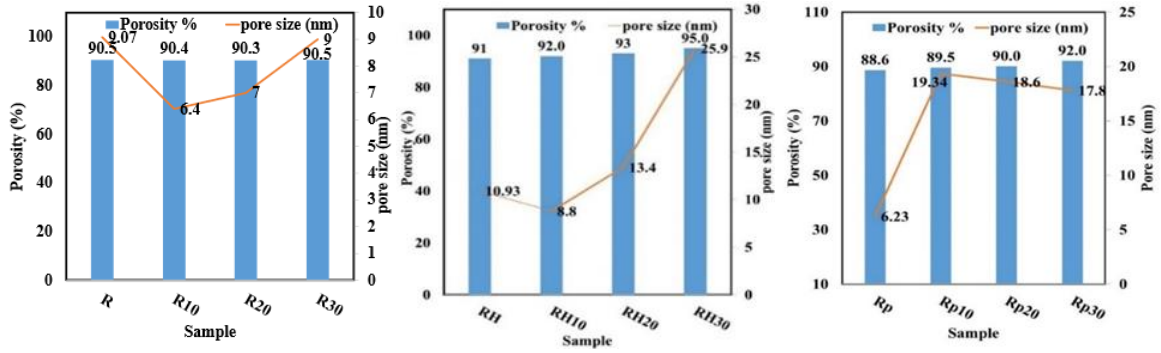

(a) (b) (c)

Figure 9. Porosity and pore size for UV raw (a), and UV chemically post-treated PVDF HFMs H_2O_2 (b), PEG (C) at different UV exposure time

including pure water permeability and MB rejection was focused on the chemically pretreated PVDF HFMs. Preliminary trials and mechanical characterization (Section 3.4) indicated that raw PVDF membranes did not exhibit sufficient mechanical stability to ensure reliable performance measurements under the combined effects of UV exposure and applied transmembrane pressure. Therefore, raw membranes were excluded from UV performance testing to maintain experimental consistency and data reliability. This approach enables a clear assessment of the relationship between UV-induced structural modifications and membrane performance without introducing uncertainty related to mechanical instability.

3.6 Water permeability and rejection

3.6.1 Pure water permeability

The pure water permeability (PWP) of H_2O_2-treated (R_H) and PEG-treated (R_P) PVDF HFMs at different UV exposure times was evaluated at varying pressures, as illustrated in Fig. 10 (a)-(b). As previously reported for the raw (R) and H_2O_2-treated (R_H) membranes [16], these samples are included here for comparison purposes.

For H_2O_2-treated membranes, water flux increased significantly with longer UV exposure, from 52.6 LMH at 10 minutes to 82.3 LMH at 30 minutes. This enhancement is attributed to the generation of reactive oxygen species (ROS) during UV irradiation, which promotes the formation of polar functional groups such as hydroxyl (-OH), carbonyl (-C=O), and carboxyl (-COOH) on the PVDF surface. These polar groups increase surface energy, enhance hydrophilicity, and potentially enlarge the effective pore size, facilitating water transport and leading to higher permeability. These observations are in agreement with previous studies on UV-irradiated PES UF TiO_2 membranes and PS/TiO_2 flat-sheet mixed-matrix membranes, which reported higher pure water flux, humic acid rejection, and complete chromium removal after short-term UV exposure. [35, 36, 58]

In contrast, the PEG-treated membrane exhibited a different behavior. Its initial PWP of 49.8 LMH decreased sharply to 25.4 LMH after 10 minutes of UV exposure, then increased slightly to 30.6 LMH at 20 minutes and reached 29.2 LMH at 30 minutes. This overall decline is noteworthy, as it occurs despite the increase in mean pore diameter (from 6.23 nm to 17.8 nm) observed in

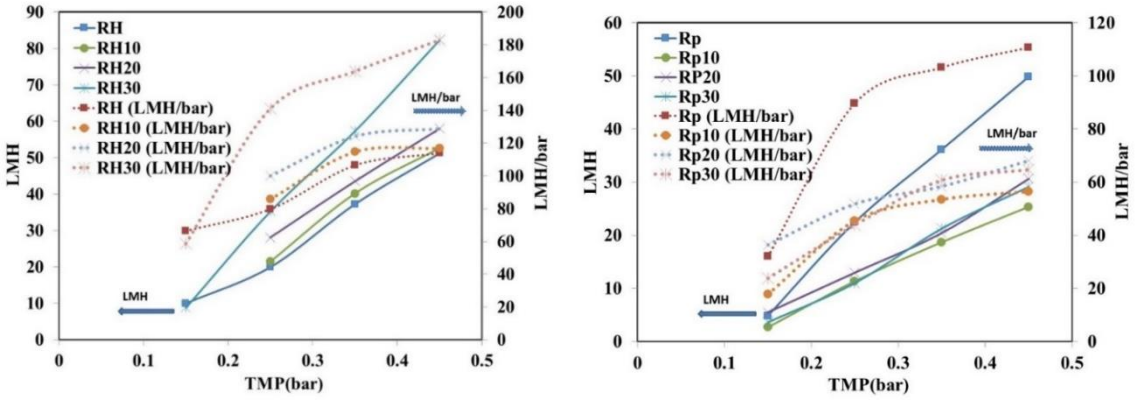

(a) (b)

Figure 10. Pure water permeability in terms of LMH, and LMH/bar for UV chemically post-treated PVDF HFMs H_2O_2 (a), and PEG (b) at different UV exposure time

Section 3.5. The reduced permeability of the PEG-treated membranes may be associated with a pore-blocking effect and surface densification. During UV irradiation, PEG residues may undergo partial redistribution, leading to obstruction of pore openings at the membrane surface. In addition, the observed reduction in wall thickness (approximately 20%) suggests structural compaction of the polymer matrix, which can increase hydraulic resistance and offset the effect of pore expansion. These results suggest that, for PEG-treated membranes, surface-related effects may play a more significant role in governing water transport than pore size alone.

Overall, these results indicate that short-term UV irradiation enhances water permeability in H_2O_2-treated membranes, while reducing it in PEG-treated membranes. The observed trends are consistent with targeted changes in surface morphology, roughness, and hydrophilicity identified in SEM, AFM, and contact angle analyses. This highlights the critical role of chemical pre-treatment in modulating the response of PVDF HFMs to UV post-treatment, allowing for a controlled approach to membrane functionalization.

3.6.2 Dye rejection

The rejection of methylene blue (MB) dye by H_2O_2-treated (R_H) and PEG-treated (R_P) PVDF HFMs exhibited distinct behaviors under different pressures (0.15–0.45 bar) and UV exposure durations (10, 20, and 30 minutes), as shown in Fig. 11(a)-(b). As previously reported for the raw (R) and H_2O_2-treated (R_H) membranes [16], these samples are included here for comparison purposes. Overall, MB rejection improved with increasing pressure after UV exposure, reaching approximately 72–75% at 0.45 bar. This indicates that while UV irradiation significantly expanded the pore size (as discussed in Section 3.5), the membranes maintained a stable and effective solute separation performance due to the synergistic effect of chemical pretreatment.

For PEG-treated membranes, R_{P10} and R_{P20} showed slightly increased rejection at higher transmembrane pressures, suggesting that moderate UV exposure enhances surface hydrophilicity and stabilizes membrane performance. In contrast, R_{P30} exhibited a slight decline in rejection at 0.45 bar, likely due to significant 20% reduction in wall thickness and substantial pore expansion observed earlier, which may slightly alter the rejection mechanism at high pressures, consistent with observations reported by Ng et al. [59]. Notably, at lower transmembrane pressures, R_{P20} and

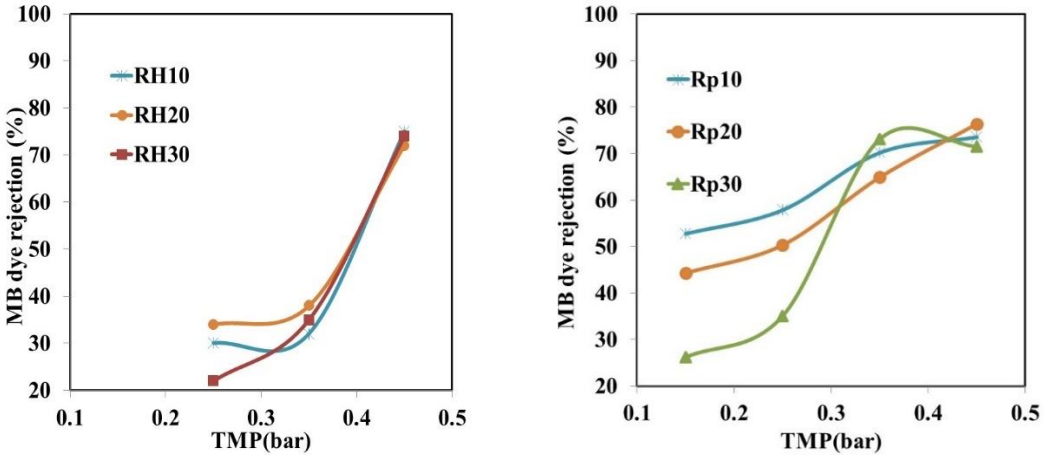

Figure 11. Rejection of Methylene blue dye for UV chemically post-treated PVDF HFMs H_2O_2 (a), and PEG (b) at different UV exposure time

R_{P30} exhibited lower MB rejection than R_{P10}. This behavior may be associated with UV-induced changes in the PEG-modified surface and minor pore deformation. Prolonged UV exposure (20–30 min) may lead to a partial loss of the PEG surface effect, reducing steric hindrance and electrostatic interactions that contribute to dye rejection under low-pressure conditions. In addition, the observed reduction in wall thickness (approximately 20%) may increase the susceptibility of these membranes to slight pore deformation at the initial stages of pressurization. At higher transmembrane pressures (>0.35 bar), MB rejection stabilized at approximately 75% for all samples, indicating that pressure-driven transport becomes dominant and minimizes the influence of surface-related effects.

Similarly, H_2O_2-treated membranes (R_{H20} and R_{H30}) showed slightly higher rejection than R_{H10} at lower pressures (0.25–0.35 bar), reflecting enhanced surface modification from combined H_2O_2 and UV treatment. Beyond 0.35 bar, all R_H and R_P membranes reached comparable rejection values (~75%), indicating that the filtration process becomes dominated by pressure-driven transport rather than surface chemistry variations.

The stability in MB rejection, despite the significant structural modifications (pore size and porosity), suggests that the surface functional groups, (–OH, –COOH) introduced by H_2O_2 and UV treatment play a crucial role in maintaining dye retention through enhanced surface affinity and electrostatic interactions. This confirms that UV post-treatment effectively enhances membrane permeability without compromising its separation capability [60].

As previously noted, the raw membrane (R) was not subjected to UV treatment for performance testing due to its observed mechanical vulnerability under UV exposure, which would preclude reliable rejection measurements under pressure [16].

4. Conclusions

The main findings of this study highlight the effects of UV post-treatment, combined with chemical pretreatments using hydrogen peroxide (H_2O_2) and polyethylene glycol (PEG), on the

structural, chemical, and performance characteristics of PVDF hollow fiber membranes. The key conclusions are:

• UV irradiation especially when combined with chemical agents (H_2O_2 and (PEG), acts as a powerful tool for significant structural reconfiguration of PVDF HFMs).

• While the bulk chemical integrity of the PVDF was preserved (as confirmed by FTIR), the treatment induced substantial physical modifications, including a significant increase in pore size and a 20% reduction in wall thickness for PEG-treated membranes.

• H_2O_2-treated membranes showed:

◦ Significant enhancement in water permeability (up to 82.3 LMH) due to increased porosity and hydrophilicity.

◦ Improved mechanical stability and the formation of hydrophilic functional groups (–OH, –COOH).

• PEG-treated membranes exhibited:

◦ Substantial structural changes, including significant pore expansion alongside a decline in water flux.

◦ The flux decline is attributed to a pore-blocking effect and surface densification/degradation (chain scission) that outweighs the impact of pore enlargement.All treated membranes maintained effective MB dye rejection with minimal variation across different UV exposure times.

• All UV-treated membranes maintained effective and stable Methylene Blue rejection (~75%), indicating that the treatment enhances permeability without compromising separation efficiency.

• UV post-treatment is confirmed as a controllable and targeted method to modify membrane properties, provided that the pretreatment agent is carefully selected to balance structural changes with performance needs.

Acknowledgements

The authors would like to thank the Ministry of International Cooperation for securing funds to initiate and support the Hollow Fibre Membranes Program at the National Research Centre from the Islamic Development Bank and Kuwait fund for Arab Economic Development.

References

1. Tavangar, T., Karimi, M., Rezakazemi, M., Reddy, K.R., Aminabhavi, T.M. (2020). Textile waste, dyes/inorganic salts separation of cerium oxide-loaded loose nanofiltration polyethersulfone membranes. Chemical Engineering Journal, 385, 123787. https://doi.org/10.1016/j.cej.2019.123787.
2. Matsuyama, H., Rajabzadeh, S., Karkhanechi, H., Jeon, S. (2017). 1.7 PVDF hollow fibers membranes. Comprehensive membrane science and engineering, 1(1.2), 137. https://doi.org/10.1016/B978-0-12-409547-2.12244-9.
3. Alkindy, M.B., Naddeo, V., Banat, F., Hasan, S.W. (2020). Synthesis of polyethersulfone (PES)/GO-SiO2 mixed matrix membranes for oily wastewater treatment. Water Science and Technology, 81 (7), 1354-1364. https://doi.org/10.1016/B978-0-12-409547-2.12244-9.
4. Yang, Z., Ma, X.H., Tang, C.Y. (2018). Recent development of novel membranes for desalination. Desalination, 434, 37-59. https://doi.org/10.1016/j.desal.2017.11.046.
5. Ho, W.W. (2003). Recent developments and applications for hollow-fiber membranes. Journal of the Chinese Institute of Chemical Engineers, 34(1), 75-89. https://doi.org/10.1016/j.memsci.2007.07.017.

6. Feng, C., Khulbe, K., Matsuura, T., Ismail, A. (2013). Recent progresses in polymeric hollow fiber membrane preparation, characterization and applications. Sep Purif Technol., 111, 43-71. https://doi.org/10.1016/j.seppur.2013.03.017
7. Huang, Y., Xiao, C., Huang, Q., Liu, H., Zhao, J. (2021). Progress on polymeric hollow fiber membrane preparation technique from the perspective of green and sustainable development. Chemical Engineering Journal, 403, 126295 http://doi.org/10.1016/j.cej.2020.126295.
8. Alkindy, M.B., Naddeo, V., Banat, F., Hasan, S.W. (2020). Synthesis of polyethersulfone (PES)/GO-SiO2 mixed matrix membranes for oily wastewater treatment. Water Sci Technology, 81(7), 1354-1364. https://doi.org/10.2166/wst.2019.347.
9. Saeedi-Jurkuyeh, A., Jafari, A.J., Kalantary, R.R., Esrafili, A. (2020). A novel synthetic thin-film nanocomposite forward osmosis membrane modified by graphene oxide and polyethylene glycol for heavy metals removal from aqueous solutions. Reactive and Functional Polymers, 146, 104397. https://doi.org/10.1016/j.reactfunctpolym.2019.104397.
10. Ren, J., McCutcheon, J.R. (2018). A new commercial biomimetic hollow fiber membrane for forward osmosis. Desalination, 442, 44-50. https://doi.org/10.1016/j.desal.2018.04.015.
11. Liang, S., Kang, Y., Tiraferri, A., Giannelis, E.P., Huang, X., Elimelech, M. (2013). Highly hydrophilic polyvinylidene fluoride (PVDF) ultrafiltration membranes via postfabrication grafting of surface-tailored silica nanoparticles. ACS Appl Mater Interfaces, 5(14), 6694-6703. https://doi.org/10.1021/am401462e.
12. Ling, R., Yu, L., Pham, T.P.T., Shao, J., Chen, J.P., Reinhard, M. (2017). The tolerance of a thin-film composite polyamide reverse osmosis membrane to hydrogen peroxide exposure. Journal of Membrane Science, 524, 529-536. https://doi.org/10.1016/j.memsci.2016.11.041.
13. Perry, L.N., Rahman, M.R., Anwar, K.M., Namakka, M., Shahabuddin, M., AlSaleem, M.S., AlHumaidi, J.Y., Rahman, M.M.(2025). Enhanced flux and surface modification of PVDF hollow fiber membranes using bamboo cellulose/PVA composite coatings, Polymer Bulletin 82, 1290912927 https://doi.org/10.1007/s00289-025-06023-8
14. Lee, J.Y., Cho, Y.H., Nam, S.E., Kim, I.C., Park, H.B., Park, Y.I., ... Yoo, Y. (2023). Surface modification of a PVDF membrane by co-grafting hydroxyl and zwitterionic polymers to enhance wettability and antifouling property. Journal of Applied Polymer Science, 140(36), e54365. https://doi.org/10.1002/app.54365
15. Saleh, S.M., Oh, P.C., Zulkifli, A.S. (2022). Surface modification of PVDF membrane via graft polymerization of acetic and acrylic acid. In IOP Conference Series: Materials Science and Engineering, 1257(1), 012032. IOP Publishing, October.
16. Sayed, E.S., Shaalan, H.F., Marzouk, M.I., Hani, H.A. (2024). Characterization and performance of post treated PVDF hollow fiber membrane. Membrane Water Treatment, 15(2), 79-88. https://doi.org/10.12989/mwt.2024.15.2.079.
17. Nasrollahi, N., Ghalamchi, L., Vatanpour, V., Khataee, A., Yousefpoor, M. (2022). Novel polymeric additives in the preparation and modification of polymeric membranes: A comprehensive review. Journal of Industrial and Engineering Chemistry, 109, 100-124. https://doi.org/10.1016/j.jiec.2022.02.036
18. Chong, M.N., Jin, B., Chow, C.W., Saint, C. (2010). Recent developments in photocatalytic water treatment technology: A review. Water Research, 44(10), 2997-3027. https://doi.org/10.3390/polym10020126.
19. Fernández, R.L., McDonald, J.A., Khan, S.J., Le-Clech, P. (2014). Removal of pharmaceuticals and endocrine disrupting chemicals by a submerged membrane photocatalysis reactor (MPR). Separation and Purification Technology, 127, 131-139. https://doi.org/10.1016/j.seppur.2014.02.031.
20. Ho, D., Vigneswaran, S., Ngo, H. (2009). Photocatalysis-membrane hybrid system for organic removal from biologically treated sewage effluent. Separation and Purification Technology, 68(2), 145-152. https://doi.org/10.1016/j.seppur.2009.04.019.
21. Molinari, R., Palmisano, L., Loddo, V., Mozia, S., Morawski, A.W. (2013). Photocatalytic membrane reactors: Configurations, performance and applications in water treatment and chemical production. In

Handbook of Membrane Reactors, 808-845. Woodhead Publishing.
22. Scott, G. (1990). Mechanisms of Polymer Degradation and Stabilisation, 170. Elsevier Applied Science, London, U.K.
23. Rupiasih, N.N., Suyanto, H., Sumadiyasa, M., Wendri, N. (2013). Study of effects of low doses UV radiation on microporous polysulfone membranes in sterilization process. Open Journal of Organic Polymer Materials, 3(1), 12-18. http://doi.org/10.4236/ojopm.2013.31003.
24. Kushwaha, S.O., Avadhani, V.C., Singh, P.R. (2014). Effect of UV rays on degradation and stability of high performance polymer membranes. Advanced Materials Letters, 5(5), 272-279. http://doi.org/10.5185/amlett.2014.10533.
25. Zhang, X., Du, A.J., Lee, P., Sun, D.D., Leckie, J.O. (2008). TiO2 nanowire membrane for concurrent filtration and photocatalytic oxidation of humic acid in water. Journal of Membrane Science, 313(1-2), 44-51. https://doi.org/10.1016/j.memsci.2007.12.045.
26. Liu, L., Liu, Z., Bai, H., Sun, D.D. (2012). Concurrent filtration and solar photocatalytic disinfection/degradation using high-performance Ag/TiO2 nanofiber membrane. Water research, 46(4), 1101-1112. https://doi.org/10.1016/j.watres.2011.12.009.
27. Aziz, S., Abu Seman, M., Saufi, S., Mohammad, A., Khayet, M. (2023). Effect of methacrylic acid monomer on UV-grafted polyethersulfone forward osmosis membrane. Membranes, 13(2), 232. https://doi.org/10.3390/membranes13020232.
28. Khan, S., Kim, J., Sotto, A., Van der Bruggen, B. (2015). Humic acid fouling in a submerged photocatalytic membrane reactor with binary TiO2–ZrO2 particles. Journal of Industrial and Engineering Chemistry, 21, 779-786 https://doi.org/10.1016/j.jiec.2014.04.012.
29. You, S.J., Semblante, G.U., Lu, S.C., Damodar, R.A., Wei, T.C. (2012). Evaluation of the antifouling and photocatalytic properties of poly (vinylidene fluoride) plasma-grafted poly (acrylic acid) membrane with self-assembled TiO2. Journal of hazardous materials, 237, 10-19. https://doi.org/10.1016/j.jhazmat.2012.07.071.
30. Rahimpour, A., Madaeni, S., Taheri, A., Mansourpanah, Y. (2008). Coupling TiO2 nanoparticles with UV irradiation for modification of polyethersulfone ultrafiltration membranes. Journal of Membrane Science, 313 (1-2), 158-169.https://doi.org/10.1016/j.memsci.2007.12.075.
31. Chin, S.S., Chiang, K., Fane, A.G. (2006). The stability of polymeric membranes in a TiO2 photocatalysis process. Journal of Membrane Science, 275 (1-2), 202-211. https://doi.org/10.1016/j.memsci.2005.09.033.
32. Tausif, A., Chandan, G. (2022). Progress in the modification of polyvinyl chloride (PVC) membranes: A performance review for wastewater treatment, Journal of Water Process Engineering, 45, 102466. https://doi.org/10.1016/j.jwpe.2021.102466
33. Siang, O.C (2015). Submerged membrane photocatalytic reactor using polyvinylidene fluoride-polyvinylpyrrolidone-titanium dioxide for oily wastewater treatment: Ph.D. Thesis, Universiti Teknologi Malaysia, Malaysia.
34. Roubaud, E., Maréchal, W., Lorain, O., Lamaa, L., Peruchon, L., Brochier, C., ... Causserand, C. (2022). Understanding aging mechanisms in the context of UV irradiation of a low fouling and self-cleaning PVDF-PVP-TiO2 hollow-fiber membrane. Membranes, 12(5), 538. https://doi.org/10.3390/membranes12050538.
35. Jyothi, M., Nayak, V., Padaki, M., Balakrishna, R.G., Ismail, A. (2014). The effect of UV irradiation on PSf/TiO2 mixed matrix membrane for chromium rejection. Desalination, 354, 189-199. https://doi.org/10.1016/j.desal.2014.10.007.
36. Mohamad, S.H., Idris, M.I., Abdullah, H.Z. (2014). Preparation of polyethersulfone ultrafiltration membrane surface coated with TiO2 nanoparticles and irradiated under UV light. Key Engineering Materials, 594, 877-881. http://doi.org/10.4028/www.scientific.net/KEM.594-595.877.
37. Kim, S.H., Kwak, S.Y., Sohn, B.H., Park, T.H. (2003). Design of TiO2 nanoparticle self-assembled aromatic polyamide thin-film-composite (TFC) membrane as an approach to solve biofouling problem. Journal of Membrane Science, 211(1), 157-165. https://doi.org/10.1016/S0376-7388(02)00418-0.
38. Madaeni, S., Ghaemi, N. (2007). Characterization of self-cleaning RO membranes coated with TiO2

particles under UV irradiation. Journal of Membrane Science, 303(1-2), 221-233 https://doi.org/10.1016/j.memsci.2007.07.017.

39. Muchtar, S., Wahab, M., Mulyati, S., Riza, M., Arahman, N. (2019). Deposition of polydopamine on the surface of Polyvinylidene Fluoride (PVDF) membrane as A UV-Shielding layer. IOP Conf Series: Mater Sci Eng; IOP Publishing. http://doi.org/10.1088/1757-899X/523/1/012017.
40. Kang, G.D., Cao, Y.M. (2014). Application and modification of poly (vinylidene fluoride)(PVDF) membranes–a review. Journal of membrane science, 463, 145-165. https://doi.org/10.1016/j.memsci.2014.03.055
41. Liu, F., Hashim, N.A., Liu, Y., Abed, M.M., Li, K. (2011). Progress in the production and modification of PVDF membranes. Journal of membrane science, 375(1-2), 1-27. https://doi.org/10.1016/j.memsci.2011.03.014
42. Wang, P., Tan, K., Kang, E., Neoh, K. (2002). Plasma-induced immobilization of poly (ethylene glycol) onto poly (vinylidene fluoride) microporous membrane. Journal of membrane science, 195 (1), 103-114. https://doi.org/10.1016/S0376-7388(01)00548-8
43. Tewfik, S.R., Sorour, M.H., Hani, H.A., Shaalan, H.F., Abulnour, A.M., El Sayed, M.M., ... Eltoukhy, M. (2022). Preparation and assessment of polyvinylidene fluoride hollow fiber membrane for desalination by membrane distillation. Desalination and Water Treatment, 255, 200-211. http://doi.org/10.5004/dwt.2022.28342.
44. Tewfik, S.R., Sorour, M.H., Shaalan, H.F., Hani, H.A., Abulnour, A.M., Sayed, E.S. (2021). Assessment of interfacial polymerization modalities on the performance of polyaniline doped polyethersulphone hollow fiber membranes. Journal of Applied Polymer Science. 138(21), 50485. https://doi.org/10.1002/app.50485.
45. Tewfik, S.R., Sorour, M.H., Shaalan, H.F., Hani, H.A., Abulnour, A.G., El Sayed, M.M., ... Eltoukhy, M.A. (2023). Effect of post-treatment routes on the performance of PVDF-TEOS hollow fiber membranes. Membrane and Water Treatment, 14(2), 85-93. https://doi.org/10.12989/mwt.2023.14.2.085.
46. Tewfik, S.R., Sorour, M.H., Shaalan, H.F., Hani, H.A. (2018). Effect of spinning parameters of polyethersulfone based hollow fiber membranes on morphological and mechanical properties. Membrane and Water Treatment, 9(1), 43-51. https://doi.org/10.12989/mwt.2018.9.1.043.
47. Sorour, M., El-Sayed, M., Moneem, N.A.E., Talaat, H.A., Shalaan, H., Marsafy, S.E. (2013). Characterization of hydrogel synthesized from natural polysaccharides blend grafted acrylamide using microwave (MW) and ultraviolet (UV) techniques. Starch-Stärke, 65(1-2), 172-178. https://doi.org/10.1002/star.201200108
48. Drioli, E., Ali, A., Simone, S., Macedonio, F., Al-Jlil, S.A., Al Shabonah, F.S., ... Criscuoli, A. (2013). Novel PVDF hollow fiber membranes for vacuum and direct contact membrane distillation applications. Separation and Purification Technology, 115, 27-38. https://doi.org/10.1016/j.seppur.2013.04.040.
49. Simone, S., Figoli, A., Criscuoli, A., Carnevale, M.C., Rosselli, A., Drioli, E. (2010). Preparation of hollow fibre membranes from PVDF/PVP blends and their application in VMD. Journal of Membrane Science, 364(1-2), 219-232. https://doi.org/10.1016/j.memsci.2010.08.013.
50. Ju, K.Y., Lee, Y., Lee, S., Park, S.B., Lee, J.K. (2011). Bioinspired polymerization of dopamine to generate melanin-like nanoparticles having an excellent free-radical-scavenging property. Biomacromolecules, 12(3), 625-632. https://doi.org/10.1021/bm101281b.
51. Lee, M.J., Ong, C.S., Lau, W.J., Ng, B.C., Ismail, A.F., Lai, S.O. (2016). Degradation of PVDF-based composite membrane and its impacts on membrane intrinsic and separation properties. Journal of Polymer Engineering, 36(3), 261-268. https://doi.org/10.1515/polyeng-2015-0064.
52. Golcuk, S., Muftuoglu, A.E., Celik, S.U., Bozkurt, A. (2013). Synthesis and characterization of polymer electrolyte membranes based on PVDF and styrene via photoinduced grafting. Journal of Polymer Research, 20(5), 144. https://doi.org/10.1007/s10965-013-0144-2.
53. Bilongo, T.G., Remigy, J.C., Clifton, M. (2010). Modification of hollow fibers by UV surface grafting. Journal of Membrane Science, 364 (1-2), 304-308. https://doi.org/10.1016/j.memsci.2010.08.024.
54. Dzinun, H., Othman, M.H.D., Ismail, A.F., Puteh, M.H., Rahman, M.A., Jaafar, J. (2017). Stability

study of PVDF/TiO2 dual layer hollow fibre membranes under long-term UV irradiation exposure. Journal of Water Process Engineering, 15, 78-82. https://doi.org/10.1016/j.jwpe.2016.05.009.

55. Baek, Y., Kang, J., Theato, P., Yoon, J. (2012). Measuring hydrophilicity of RO membranes by contact angles via sessile drop and captive bubble method: A comparative study. Desalination, 303, 23-28. https://doi.org/10.1016/j.desal.2012.07.006.
56. Wang, L., Wei, J., Wu, B. (2016). Enhancing hydrophilicity performance of polysulfone hollow fiber membrane by surface modification via UV-induced graft polymerization of HEA. Desalination and Water Treatment, 57 (35), 16269-16276. https://doi.org/10.1080/19443994.2015.1081628.
57. Rahimpour, A. (2011). UV photo-grafting of hydrophilic monomers onto the surface of nano-porous PES membranes for improving surface properties. Desalination, 265 (1-3), 93-101. https://doi.org/10.1016/j.desal.2010.07.037.
58. Vatanpour, V., Hazrati, M., Sheydaei, M., & Dehqan, A. (2022). Investigation of using UV/H2O2 pre-treatment process on filterability and fouling reduction of PVDF/TiO2 nanocomposite ultrafiltration membrane. Chemical Engineering and Processing-Process Intensification, 170, 108677. https://doi.org/10.1016/j.cep.2021.108677.
59. Ng, L.Y., Ahmad, A., Mohammad, A.W. (2017). Alteration of polyethersulphone membranes through UV-induced modification using various materials: A brief review. Arabian Journal of Chemistry, 10, S1821-S1834. https://doi.org/10.1016/j.arabjc.2013.07.009.
60. Tang, S., Deng, Y., Wang, Y., Tang, T., Luo, H., Zhang, X. (2025). Hydrogen peroxide immersion for efficient cleaning of fouled manganese-doped ceramic membranes in wastewater treatment. Separation and Purification Technology, 361, 131357. https://doi.org/10.1016/j.seppur.2024.131357.